Food Chemistry 377 (2022) 132072

Contents lists available at ScienceDirect

Food Chemistry

journal homepage: www.elsevier.com/locate/foodchem

A competitive colorimetric aptasensor for simple and sensitive detection of kanamycin based on terminal deoxynucleotidyl transferase-mediated signal amplification strategy

Tingting Zhao [a,1], Qian Chen [a,1], Yanli Wen [b], Xiaojun Bian [a], Qing Tao [a], Gang Liu [b], Juan Yan [a,*]

[a] Laboratory of Quality and Safety Risk Assessment for Aquatic Products on Storage and Preservation (Shanghai), Ministry of Agriculture Shanghai Engineering Research Center of Aquatic-Product Process & Preservation, College of Food Science and Technology, Shanghai Ocean University, Shanghai 201306, China
[b] Laboratory of Biometrology, Division of Chemistry and Ionizing Radiation Measurement Technology, Shanghai Institute of Measurement and Testing Technology, Shanghai 201203, China

ARTICLE INFO

Keywords:
Aptamer
Biosensor
Signal amplification strategy
Magnetic beads
Antibiotic residues
Food safety

ABSTRACT

We developed a rapid and sensitive colorimetric biosensor based on competitive recognition between kanamycin (KAN), magnetic beads-kanamycin (MBs-KAN) and aptamer and terminal deoxynucleotidyl transferase (TdT)-mediated signal amplification strategy. In the absence of KAN, aptamers recognize MBs-KAN. TdT can amplify oligonucleotides to the 3′-OH ends of aptamers, with biotin-dUTP being embedded in the long single stranded DNA (ssDNA). Then the assay produced visual readout due to the horseradish peroxidase (HRP)-catalyzed color change of the substrate after the linkage between biotin and streptavidin (SA)-HRP. In the presence of KAN, however, aptamers tend to bind free KAN rather than MBs-KAN. In this case, aptamers are isolated by magnetic separation, resulting in the failure of signal amplification and catalytic signals. This competitive colorimetric sensor showed excellent selectivity toward KAN with the limit of detection (LOD) as low as 9 pM. And recovery values were between 93.8 and 107.8% when spiked KAN in milk and honey samples.

1. Introduction

Kanamycin (KAN), a basic aminoglycoside antibiotic produced by Streptomyces Kanamyceticus, possesses the ability of blocking the synthesis of proteins to achieve the treatment of severe infections of Gram-positive and Gram-negative bacteria (Feng et al., 2019). Therefore, KAN has become a common veterinary drug in poultry and aquaculture. However, unreasonable, or excessive use of KAN may cause it to remain in animal-derived food (e.g., milk, honey, eggs, and meat) and eventually enter the human body through the biological circulation system, resulting in serious side effects to human health such as loss of hearing, kidney toxicity and allergic reactions (Bai et al., 2019), as well as potential harm to the environment. Recently, KAN residue has become a serious public health issue on a global scale (Lin et al., 2019). The European Commission has established maximum residue limits (MRLs) for KAN in different foods, for instance, 150 μg/kg for milk, 100 μg/kg for fat and muscle (Commission, 2010). China has also set MRLs of 200 μg/kg for KAN in milk. As a matter of fact, long-term consumption of food even at a much lower-level antibiotic than reported MRLs values, has still been reported to cause many adverse side effects in humans. Therefore, it is necessary to develop a sensitive and specific method for quantitative detection of KAN.

At present, a variety of methods have been proposed for the detection and analysis of KAN residue, such as high-performance liquid chromatography (HPLC) (Zhang et al., 2019), high performance liquid chromatography tandem mass spectrometry (HPLC-MS) (Perez, & Chen, 2018), surface plasmon resonance (SPR) (Zhang et al., 2018), enzyme-linked immunosorbent assay (ELISA) (Li et al., 2017) and so on. Although those conventional measures exhibit their own advantages, they may still be limited by unsatisfactory detection sensitivity, the need for large, sophisticated laboratory instruments, time-consuming steps, and high requirements for operators (Cheng et al., 2020). Thus, it is urgent to develop novel sensitive, simple, and rapid strategies suitable for on-site food safety screening to solve these issues.

In recent years, a variety of biosensing solutions for food safety monitoring have been proposed (Zhou et al. 2021) and implemented

* Corresponding author.
E-mail address: j-yan@shou.edu.cn (J. Yan).
[1] These authors contributed equally to this work.

https://doi.org/10.1016/j.foodchem.2022.132072
Received 17 May 2021; Received in revised form 19 November 2021; Accepted 3 January 2022
Available online 5 January 2022

properly in the regimes of aptamer-based biosensors (aptasensors) (Cheng et al., 2020; Zhu et al., 2021). Aptamers are single-stranded oligonucleotides sequence, obtained from vitro nucleic acid molecular library through a procedure called systematic evolution of ligands by exponential enrichment (SELEX) (Tuerk, & Gold, 1990), which can bind to a number of different targets such as ions, small molecules, proteins and cells with high affinity and specificity (Zhu et al., 2012). Due to the inherent advantages of high stability, easy storage, low cost, convenient synthesis, and modification (Wang et al., 2017), various aptasensors have been developed and attracted considerable attention in food monitoring and control (Song et al., 2008), such as colorimetric (Liu, Yang, Li, & Du, 2021), fluorescence (Ramezani et al., 2016), electrochemical (Zhou et al., 2019) and electrochemiluminescence (Cheng et al., 2020). Among these aptasensors, colorimetric has been used extensively due to its low cost, simplicity, practicality, and observation of the color change by the naked eyes without any sophisticated instruments (Cheng, Liu, Shi, & Zhao, 2018). So far, numerous different colorimetric aptasensors have been constructed based on the characteristic of the structure conversion of KAN aptamer (Birader et al., 2021; Wu et al., 2020; Ha et al., 2017; Robati et al., 2016; Xu et al., 2015). Nevertheless, these traditional colorimetric aptasensors are typically restricted by their moderate sensitivity, as well as detection specificity when they are adopted in complicated food matrices.

For the purpose of improving the sensitivity of DNA-based biosensors, numerous nucleic acid signal amplification strategies have been developed, such as polymerase chain reaction (PCR) (Shen et al., 2021), rolling circle amplification (RCA) (Du et al., 2019), hybrid chain reaction (HCR) (Li et al., 2019) and so on. However, heavy dependence on temperature control devices limits the wide application of PCR for point of on-site detection. Meanwhile, RCA and HCR often involve complicated DNA sequence template or complex probe design process. Terminal deoxynucleotidyl transferase (TdT)-mediated amplification, however, is a template-free DNA strand extension reaction without strict temperature control, providing a possible option for developing novel biosensors suitable for on-site food safety screening (Guo et al., 2018; Tian et al., 2020).

Herein, to adapt the joint merit of TdT amplification and aptamers, a TdT amplification-based and magnetic beads (MBs)-assisted competitive colorimetric aptasensor for highly sensitive and simple detection of KAN was proposed. In the absence of target KAN, KAN molecules that were pre-immobilized on MBs recognized aptamers in solution and the strong catalytic colorimetric signal was detected with recourse to TdT-directed polymerization. When the target KAN was in the presence, however, those KAN would competitively bind to the aptamers and the aptamers were subsequently removed from the supernatant through magnetic separation, resulting in the failure of amplification and signals generation. Overall, given the fusion across competitive binding assay, colorimetric strategy, MBs-facilitated separation and TdT amplification, the proposed detection method for KAN may find great potential in the future for simple and ultrasensitive detection of other antibiotics residue in the field of food safety.

2. Materials and methods

2.1. Reagents and chemicals

The HPLC-purified oligonucleotides used in this paper were purchased from Shanghai Sangon Biotechnology Co., Ltd. (Shanghai, China). The sequences of them were as follows. KAN aptamer: 5′-TGG GGG TTG AGG CTA AGC CGA GTC AC-3′; Biotin labeled KAN aptamer: 5′-Biotin-TTT TTT TTT TTG GGG GTT GAG GCT AAG CCG AGT CAC-3′. Terminal deoxynucleotide transferase (TdT) and TdT buffer were supplied by Beyotime Biotechnology Co., Ltd. (Shanghai, China). Bio-Mag®Plus Amine modified magnetic beads (MBs, 50 mg/mL) and magnetic separator were purchased from Polysciences Inc (USA). 1-ethyl-3- (3-dimethylaminopropyl) carbodiimide hydrochloride (EDC) was obtained from Sigma-Aldrich Chemical Co., Ltd. (Shanghai, China). Phosphate buffered saline (PBS, 20 ×, pH 7.4), Agarose, 25 base-pair ladder Marker, Tris-HCl buffer (20 mM, pH 7.0), casein, Biotin-11-dUTP (1 mM), Kanamycin (KAN), Streptomycin (STR), Chloramphenicol (CAP), Tetracycline (TET), Ofloxacin (OFX), and Lincomycin (LIN) were obtained from Shanghai Sangon Biotechnology Co., Ltd. (Shanghai, China). Bovine serum albumin (BSA) was purchased from Amresco (USA). 3, 3′, 5, 5′-tetramethylbenzidine (TMB) was obtained from Neogen (USA). Streptavidin-labeled horseradish peroxidase (SA-HRP) was provided by Thermo Fisher Scientific Co., Ltd. (Shanghai, China). 2-Morpholinoethanesulfonic acid (MES) was bought from Aladdin Reagent Co., Ltd. (Shanghai, China). All other reagents were analytical grade and were used without further purification. Millipore purification system-based ultrapure water was used in this study (18.2 MΩ cm, Milli-Q, Millipore).

2.2. Apparatus

The UV–vis spectra were recorded by a UV-2540 spectrophotometer (Shimazu Co., Japan). Fourier transform infrared (FT-IR) spectra were recorded by a Nicolet 6700 FT-IR spectrophotometer (Madison, Wisconsin, USA). The transmission electron microscopic (TEM) image was obtained from a FEI Talos F200X G2 field emission transmission electron microscope (USA). Synergy2 SLFPTAD multi-functional microplate reader was obtained from Boten Instrument Co., Ltd. (USA). HCM100-Pro constant temperature oscillating metal bath and D1008 handheld centrifuge were provided by Dalong Xingchuang Experimental Instrument Co., Ltd. (Beijing, China). Agarose gel images were recorded by BIO-RAD Gel Doc XR imaging analysis system (USA). All atomic force micrographs (AFM) were obtained using a Bruker Dimension FastScan Bio (Germany).

2.3. Preparation of aldehyde modified MBs

The preparation of aldehyde modified magnetic beads was performed as follow. Firstly, 2 mL of amino-modified magnetic beads were added into 16 mL of 10 mM pyridine buffer solution in a 50 mL centrifuge tube, and vigorously stirred for 15 mins. Then the supernatant was discarded with a magnetic field. The precipitate was repeatedly washed with pyridine buffer solution for three times. After that, 8 mL of 5% glutaraldehyde solution was added and the mixture was shaken at 25 °C for 3 h. Next, the mixed solution was subjected to magnetic separation and the supernatant was abandoned. The precipitate was repeatedly washed with 16 mL of pyridine buffer until the solution was clear. Finally, 2 mL of 10 mM PBS solution was added into the precipitate and stored at 4 °C.

2.4. Preparation of MBs-KAN complex

A carbodiimide crosslink method was used to prepare MBs-KAN (Park et al., 2015) and the preparation procedures were as follows. The supernatant of 400 μL (20 mg) of aldehyde modified magnetic beads was magnetically separated and the precipitate was washed with 2 mL of MES coupling solution (20 mM) for three times. Then the mixture of 2 mL of MES coupling solution and 2 mL of EDC solution (20 mg/mL) was added to the precipitate and incubated for 3 h at room temperature in the dark. The above washing procedures were repeated three times. After that, 4 mL of KAN (100 g/L) was added to the precipitate and incubated overnight at room temperature in the dark. Completely removed the supernatant with washing buffer (1 mM PBS, 1 mM $MgCl_2$, 0.05% Tween-20, pH 7.4) for three times, adding 2 mL of PBS buffer (10 mM, containing 2% BSA) into the precipitate. The obtained MBs-KAN was stored at 4 °C in the dark.

2.5. Preparation of TdT-based colorimetric KAN aptasensor

The supernatant of 5 μL of MBs-KAN solution was magnetically removed. 20 μL of KAN aptamer (500 nM) and 20 μL of KAN solution was added into the precipitate simultaneously. After 1 h of incubation at room temperature, the conjugates were rinsed with buffer (50 mM Tris-HCl, pH 7.4). Then 20 μL of a mixed TdT reaction solution containing TdT buffer (5×, 4 μL), terminal deoxynucleotidyl transferase (20 U/μL, 2 μL), Biotin-dUTP (1 mM, 1 μL), dNTPs (1 mM, 1 μL) and Tris-HCl buffer (50 mM, 8 μL) was added to the precipitate and incubated for 30 min at 37 °C. Then rinsed the TdT amplification products with Tris-HCl buffer for three times. After blocking with 4% BSA for 30 min, 2 μL of a 1000-fold diluted SA-HRP was added to the precipitate and incubated at 25 °C for 20 min. The conjugates were then rinsed with washing buffer (1 mM PBS, 1 mM $MgCl_2$, 0.05% Tween-20, pH 7.4) for six times, adding 50 μL of TMB solution to the precipitate. After the incubation at 37 °C for 5 min, the absorption values of blue products in the supernatant were measured at a wavelength of 652 nm in a 96-well plate (Greiner).

2.6. Detection of KAN in real food samples with TdT-based colorimetric aptasensor

Real food samples were purchased from a local supermarket (Shanghai, China). 2 mL milk sample were diluted with PBS buffer (10-fold dilution). The milk samples were centrifuged at 11000 rpm for 25 min at 4 °C and removed the precipitate. The supernatant was filtered through a 0.22 μm membrane and the filtrate was collected. The sample of honey was diluted with PBS water (5-fold dilution). A series of KAN standard solutions were spiked to milk and honey samples.

3. Results and discussion

3.1. The working principle of TdT-based colorimetric aptasensor for KAN

The principle of visual strategy for KAN detection is illustrated in Scheme 1. The proposed assay system mainly consists of competitive molecular recognition event, enzymatically catalytic signal amplification and catalytically chromogenic reaction. All the procedures are designed to occur on the surface of MBs with the advantages of simplicity, low cost and easy to functionalize (Sadasivam et al., 2020).

To construct the MBs complex, KAN are immobilized onto the surfaces of aldehyde based MBs using carbodiimide crosslinking. Although those pre-immobilized KAN and free target KAN competitively bind to aptamers, the latter holds prominent binding superiority due to its relatively smaller steric hindrance effect. In the absence of KAN, aptamers bind specifically to KAN immobilized on the MBs with high affinity. When the mixture of TdT, dNTPs and biotin-dUTP are added, TdT catalyzes the sequential extension of deoxyribonucleoside at 3′-OH terminals of aptamers without any templates, generating long single-stranded DNA (ssDNA) products embedded with biotin sites. Following the introduction of SA-HRP, HPR molecules are incorporated into the ssDNA chains through biotin-SA combination. Finally, HRP catalyzes the H_2O_2-mediated oxidation of TMB and forms a blue chromogenic product for the colorimetric assay (Yan et al., 2010). In the presence of excess free target KAN, however, aptamers preferably bind to free KAN and the aptamers are almost consumed, which are subsequently removed by the magnetic separation. This means no 3′-OH terminals left for the subsequent amplification and, therefore, leads to no valid signals. With the decrease of the concentration of free target KAN, the number of aptamers remaining that recognize KAN immobilized on MBs rises, resulting in the increase of the signals. Hence, there is a negative correlation between the free target KAN concentration and the colorimetric signal.

3.2. Characterization of MBs complexes

Amino-MBs were firstly treated to produce Aldehyde-MBs, and the modified particles were then measured with a Fourier transform infrared (FT-IR) spectroscopy. As shown in Fig. 1A, the characteristic bands of Amino-MBs were observed at 3430 cm^{-1} (N—H stretch vibrations), 1630 cm^{-1} (N—H bending vibrations) and 580 cm^{-1} (Fe-O vibration) (Sadasivam et al., 2020). After the modification, the characteristic bands of the Aldehyde-MBs were found at 2930 cm^{-1} (C—H stretch vibrations) and 1750 cm^{-1} (-C═O vibration) respectively (Zhang, Wang, Wang, & Yang, 2010), indicating that the glutaraldehyde was successfully coated on the MBs. Furthermore, after the linkage between KAN and Aldehyde-MBs, the products were also characterized by FTIR. In Fig. 1B, the absorption peaks at 1600 cm^{-1} and 1080 cm^{-1} were subject to N—H bending vibration and C—O stretching vibration of KAN, respectively. Compared with Aldehyde-MBs, the peak at 1150 cm^{-1} (C—N stretching vibrations) of MBs-KAN became more obvious. And a C—N—C asymmetric stretching vibration was present at 1390 cm^{-1}. These data were consistent with the literature (Qiu et al., 2020) and suggested that KAN was successfully immobilized on the surface of Aldehyde-MBs.

The successfully specific recognition of the aptamers to the targets

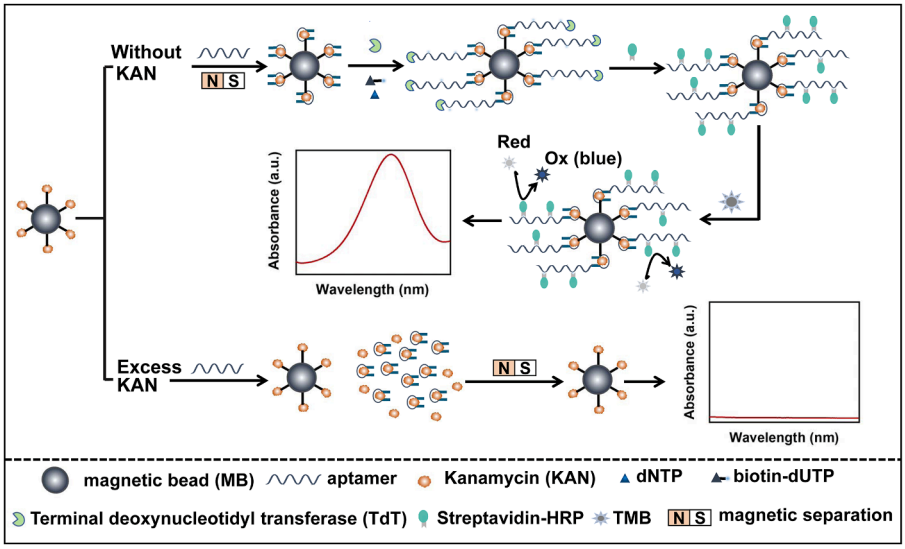

Scheme 1. Schematic illustration of terminal deoxynucleotidyl transferase (TdT)-based competitive colorimetric aptasensor for KAN.

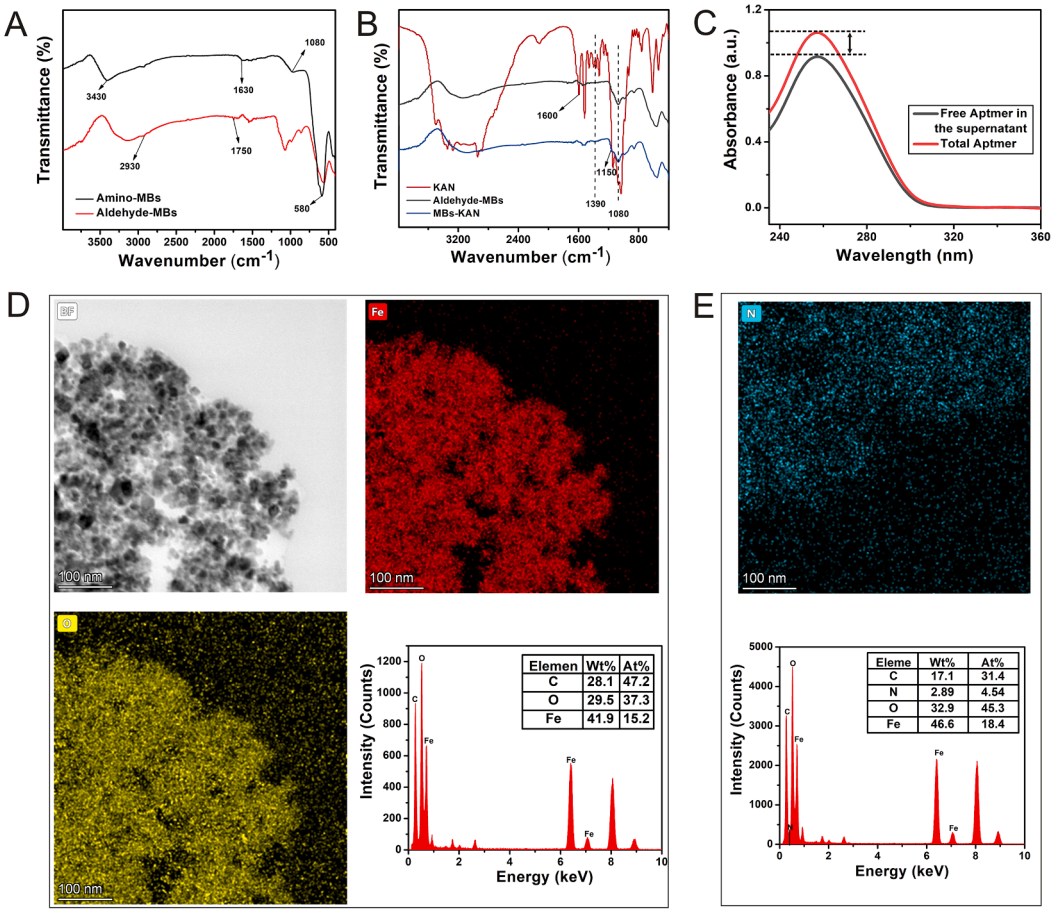

Fig. 1. (A) FTIR spectra of Amino-MBs and Aldehyde-MBs. (B) FTIR spectra of KAN, Aldehyde-MBs and MBs-KAN. (C) Quantification results of the aptamer in solution before (red line) and after (black line) the recognition between aptamers and MBs-KAN complexes. (D-E): Field emission transmission electron microscope energy-dispersive spectroscopy (FETEM-EDS) results of Ultrathin frozen sections of MBs complexes. (D) Electron bright field image, EDS elemental mapping images of Fe (red) and O (yellow) and EDS spectra of CHO-MBs. (E) EDS elemental mapping images of N (blue) and EDS spectra of MBs-KAN. (For interpretation of the references to color in this figure legend, the reader is referred to the web version of this article.)

was recognized as the critical procedure for aptasensor, especially when the aptamer functioned as the primer to initiate TdT-based signal amplification in the work. Therefore, the recognition between aptamers and KAN was firstly investigated. The absorbance spectrum of aptamer before and after recognition was compared, as shown in Fig. 1C, the concentration of free DNA decreased obviously, demonstrating the fact that considerable amounts of aptamers combined onto the surface of MBs-KAN complex when they met with pre-immobilized KAN.

Field emission transmission electron microscope (FETEM) and energy dispersive spectroscopy (EDS) elemental mapping analysis were also used to study the product of each step. In Fig. 1D, electron bright field of ultrathin section, elemental mapping images and EDS spectra were displayed, respectively. Fe (red) and O elements (yellow) from MBs were evenly distributed in images, showing the composition of CHO-MBs which was confirmed further by the EDS intensity data. Meanwhile, since the molecular composition of KAN is C, H and N elements, the presence of N elements (blue) in Fig. 1E confirmed the successful fixation of KAN on activated MBs. Other EDS images of MBs-KAN can be found in Fig. S1.

3.3. Verification of TdT-based DNA amplification

TdT can catalyze the extension of DNA at the 3′-OH terminals without the assistance of a template. Free aptamers were first amplified in solution using TdT and dNTPs and TdT products were characterized by agarose gel electrophoresis. As shown in Fig. 2A, amplified DNA products showed increased molecular weight (lane 2, Fig. 2A) than aptamers without extension (lane 1, Fig. 2A). Atomic force microscopy (AFM) images in Fig. 2B provided more intuitive evidence for TdT amplification, where strands of DNA were found for TdT products (left) and no obvious DNA strand for the control group (right). These data demonstrated the successful TdT amplification of aptamer in solution. In addition, it can also be seen that TdT-generated single-stranded DNA (ssDNA) (green arrow) tended to entangle with each other due to its flexible property and formed partial unspecific double-stranded DNA (dsDNA) (yellow arrow). This characteristic of TdT-generated ssDNA was the same as that of RCA-produced ssDNA shown in our previous work (Yan et al., 2015) The difference was that the chain length by RCA amplification could reach micro scale, while the DNA chains amplified by TdT reaction was much shorter. The reason for this has been attributed to the different amplification efficiencies of TdTase and phi29 polymerase.

Next, TdT amplification was performed further on the surface of MBs, and the products were similarly verified by the technique of EDS. The corresponding EDS mapping and analysis results were shown in **Fig. S2** and Fig. 2C. Results showed the distribution of P elements (purple) appeared after the amplification. It is well known that nucleic acids are formed by the polymerization of multiple nucleotides by 3′, 5′-phosphodiester bonds. Accordingly, the distribution of P elements meant the presence of DNA on MBs. Moreover, compared with other element evenly distributed mapping images, there were two distinct purple spots in Fig. 2C (left), probably because TdT-produced ssDNA got

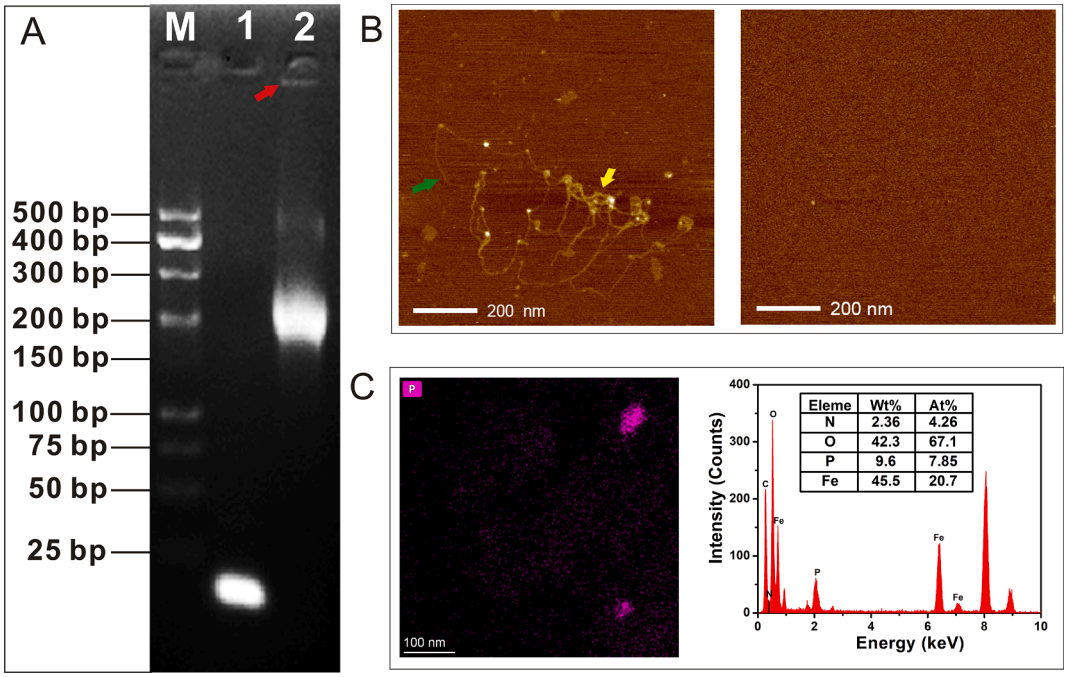

Fig. 2. (A) Image of agarose gel electrophoretic analysis of TdT products. M: 25 bp ladder DNA marker, lane 1 was aptamer and lane 2 was TdT-produced ssDNA. (B) AFM characterization results of TdT-produced ssDNA (left) and the aptamer (right). Height scales were 5 nm. Green arrow: ssDNA; Yellow arrow: partial double-stranded DNA (dsDNA) because of DNA-DNA unspecific interactions. (C) EDS elemental mapping images of P (purple) and EDS spectra of MBs-ssDNA. (For interpretation of the references to color in this figure legend, the reader is referred to the web version of this article.)

tangled up in one place and aggregated together, creating bright spots of P elements in the mapping image. These results verified the feasibility of TdT-based signal amplification strategy on the surface of MBs.

3.4. Construction and optimization of TdT-based colorimetric aptasensor for KAN

Based on the verification of TdT extension on MBs above, the detection ability of TdT-based aptasensor for KAN was then studied. During the TdT extension, biotin sites were introduced into TdT-generated long ssDNA via the use of biotin-dUTP, which specifically reacted with SA-HRP and subsequently produced colorimetric signal for quantitative analysis (Yan et al., 2018). As shown in Fig. S3A, the absorbance reading out by TdT amplification was significantly higher than that of control group (without TdT reaction), demonstrating a good signal-to-background ratio of the aptasensor. Furthermore, in the presence of KAN (500 nM), negligible absorbance intensity at 652 nm was observed while that of blank group (without KAN) showed a strong absorption peak at 652 nm (Fig. S3B). These data confirmed the fact that free target KAN molecules held prominent superiority over those immobilized on the surface of MBs in competitive binding of aptamers in solution. The change in absorbance at 652 nm was monitored for subsequent quantitative analysis of KAN.

Next, to achieve the best performance of the assay, several experimental parameters were optimized in terms of amount of MBs, aptamer concentration, incubation time, and TdT amplification time before the investigation of the detection capability of the aptasensor for KAN. First, the amount of MBs was critical for the detection ability of TdT-based aptasensor. The reason was that if the amount of MBs was too small to meet the binding requirement of all free aptamers, the number of aptamers on the MBs which were used to initiate TdT amplification was limited, resulting in a low signal. As shown in Fig. S4A, the optimum amount of MBs-KAN was 50 μg.

Similarly, the number of aptamers, the incubation time among aptamer, free KAN, and MBs-KAN, and TdT extension time were optimized in turn. As shown in Fig. S4B, the highest ΔA was found at the aptamer concentration 500 nM. As displayed in Fig. S4C and Fig. S4D, the optimum incubation time of aptamer, KAN and MBs-KAN was obtained at 60 min and the TdT amplification time was obtained at 40 min. The statistical analysis in Fig. S5 confirmed these optimizations, compared to control treatments. It should be noted that the absorbance intensity change (ΔA) was applied for the quantitative analysis of KAN in the work. The calculation of ΔA value was based on the following formula (Tian, Zhou, Jiao, & He, 2019):

$$\Delta A = A_0 - A_S$$

Where A_0 represented the absorbance intensity of ox TMB at 652 nm in the absence of KAN, while A_S referred to absorption values of samples.

3.5. Performance of TdT-based colorimetric aptasensor for KAN detection

The sensitivity of this aptasensor was finally verified through analysis of a series of KAN standard solutions under the optimized experimental conditions. With the increase of KAN concentration (from 0.01 nM to 500 nM), different shades of blue chromogenic product were conveniently observed subjected to the natural light, demonstrating the visual detection capability of the sensor for KAN (Fig. 3A). Meanwhile, the maximum absorption peak at 652 nm decreased responsively with the increase in KAN concentrations (Fig. 3B). There was a clear correspondence between the KAN concentration and absorption (Fig. 3C). In addition, the ΔA_{652} showed a good linear relationship with the KAN concentrations in the range from 0.01 to 500 nM ($Y = 0.1895X + 0.6038$, $R^2 = 0.9937$) (Fig. 3D). Statistical analysis revealed that for the limit of detection (LOD), the TdT-based colorimetric aptasensor was equal to 9 pM, as estimated by using $LOD = 3\sigma/S$, where σ was the relative standard deviation of a blank solution, S was the slope of the calibrated curve.

Additionally, a common biotin-aptamer-based colorimetric procedure for KAN (Fig. 4A) gave rise to insignificant ΔA_{652}, in stark contrast to those signals produced by TdT-based aptasensor (Fig. 4B and Fig. S6A). The sensitivity of this method was far better than acceptable limits set by the European Union and China for KAN detection. Moreover, the

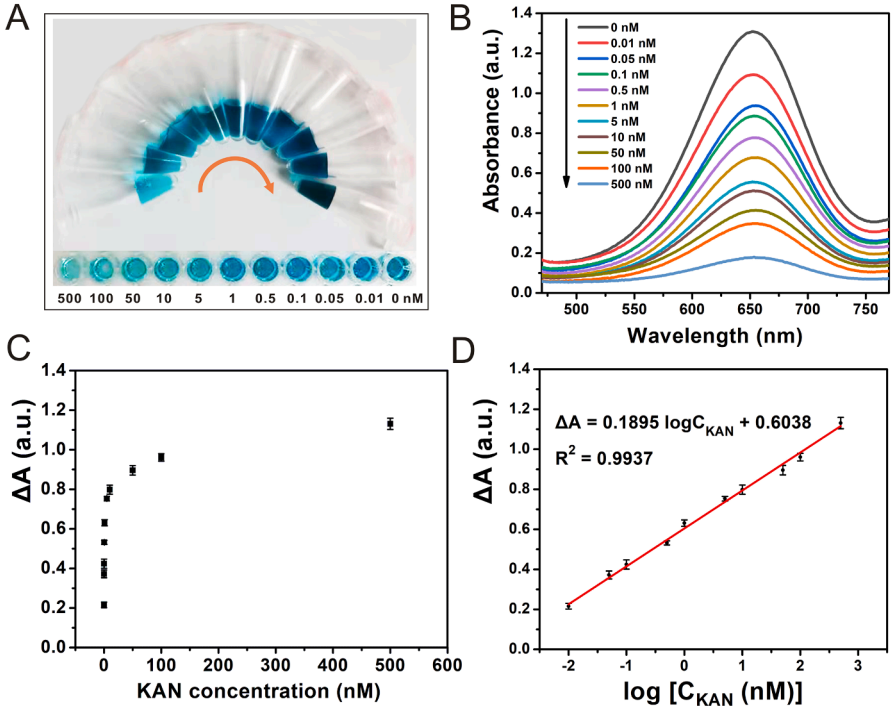

Fig. 3. (A) Photograph of aptasensor with various concentrations of KAN. (B) UV–vis absorption spectra at 652 nm of the system with different concentrations of KAN (0, 0.01, 0.05, 0.1, 0.5, 1, 5, 10, 50, 100, 500 nM). (C) Correspondence between the KAN concentration and absorption value. (D) The linear relationship between the absorbance intensity changes at 652 nm and the KAN concentration. The error bars illustrate the standard deviations of three replicate measurements.

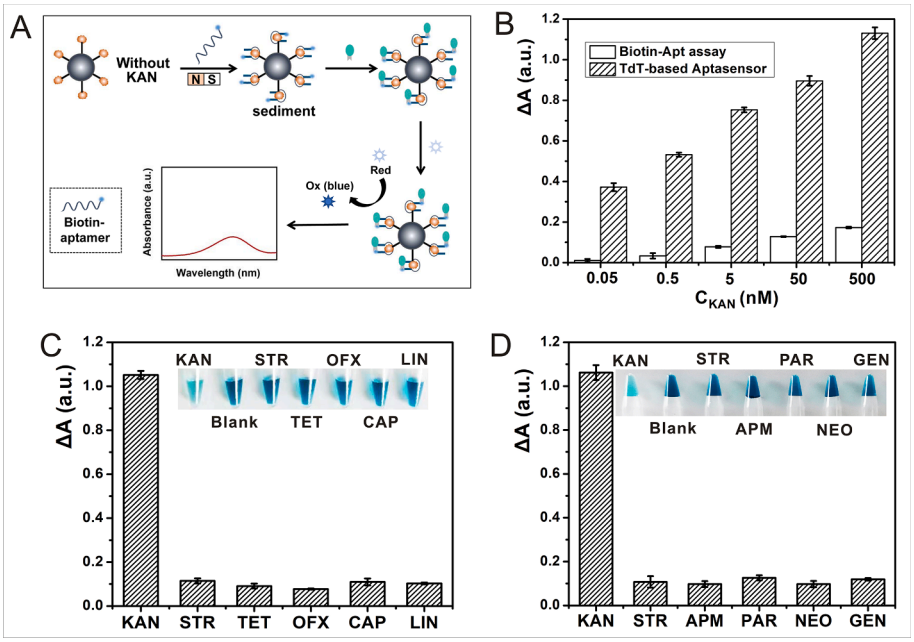

Fig. 4. (A) Scheme of biotin-aptamer colorimetric assay for the detection of KAN. (B) Comparison of KAN analysis signals between methods of biotin-aptamer assay and TdT-based aptasensor. (C) The selectivity of the colorimetric aptasensor for KAN among common antibiotics (KAN: 500 nM; Controls: 5 μM). (D) The selectivity of the colorimetric aptasensor for KAN comparing with other aminoglycoside antibiotics (KAN: 500 nM; Controls: 5 μM).

sensitivity of this sensor is three orders of magnitude higher than that of the commercially available Kanamycin ELISA kit (for milk and honey samples) whose LOD is only 3.1 nM. To exemplify the competency of the TdT-based colorimetric aptasensor in KAN analysis, a crosswise comparison was carried out among commonly available technologies in Table S1, for instance, HPLC-MS, Surface-enhanced Raman Scattering (SERS), Fluorescence, Electrochemistry, RCA-based microfluidic strategy, and colorimetry, *etc*.. It is obvious that the detection sensitivity of this method is superior to most of the listed KAN detection strategies. Although super high sensitivity could be achieved by combining RCA technique (He et al., 2019) or exonuclease I-assisted signal amplification (Li et al., 2021), it demanded strictly timed protocols including the design, preparation, and the hybridization of circular DNA template, or may be affected by complex food matrices. The TdT-based colorimetric

strategy serves predominantly as an expedient measure over the others in on-site KAN indication. From the above data and comparison, the prominent detection sensitivity of this method could be attributed to TdT amplification, which can significantly improve the amount of HRP in the catalytic system.

The specificity of the method was also demonstrated by analyzing 500 nM KAN together with five other kinds of antibiotics, including Streptomycin (STR), Tetracycline (TET), Ofloxacin (OFX), Chloramphenicol (CAP) and Lincomycin (LIN). Although the concentration of every unspecific antibiotic was 10 times higher than KAN, there was none of them inducing a remarkable ΔA_{652} and color change as KAN did (Fig. 4C and Fig. S6B). Furthermore, the selectivity of the method was also be checked by studying other aminoglycoside antibiotics such as Streptomycin (STR), Apramycin (APM), Paromomycin (PAR), Neomycin (NEO), and Gentamicin (GEN) in addition to the above commonly encountered antibiotics, and the results were shown in Fig. 4D and Fig. S6C. The response signal generated by KAN (ΔA_{652}) was the most sensitive in comparison with that of other control groups. These results clearly exhibited excellent selectivity of the designed aptasensor for the detection of KAN.

3.6. Determination of KAN in real food samples

Finally, to further evaluate the accuracy and applicability of the assay for the real sample analysis, different concentrations of KAN were spiked into the blank milk and honey samples (0.5, 1, 5 nM, respectively). The recoveries were from 93.8% to 107.8% with relative standard deviations (RSDs) of 1.22%–4.39% (<5%) (Table 1), indicating acceptable accuracy and precision of the aptasensor for KAN, as well as the feasibility of being applied for actual food samples analysis.

4. Conclusions

In summary, an innovative competitively colorimetric biosensing assay for KAN was established. Compared with the existing similar aptasensing strategies, highlights of the work mainly focus on the following issues. (1) The method is simple, highly sensitive and can be implemented in a variety of non-laboratory settings. TdT amplification contributes to the highly sensitive detection but does not require strict temperature control and complex experimental design required by other typical nucleic acid signal amplification technologies. More importantly, TdT-assisted DNA extension can be well combined with colorimetric strategy, which is suitable for the development of on-site detection methods. (2) MBs used in the work not only facilitate to simplify the operation, but also effectively eliminate the potential interferences in complex food matrices, thus combining with the specific aptamer to achieve high selective assay. (3) The assembly of KAN on the surface of MBs via covalent linkage guarantees its good structural stability, providing the possibility for commercial availability. Additionally, this TdT-based colorimetric aptasensor has an immense potential for other targets detection through the replacement of the MBs complexes and the corresponding aptamers, which may provide its broadly application prospects for visual detection in food security, environmental monitoring, and disease diagnosis.

CRediT authorship contribution statement

Tingting Zhao: Conceptualization, Methodology, Investigation, Software, Data curation, Writing – original draft. **Qian Chen:** Methodology, Software, Data curation, Validation. **Yanli Wen:** Software, Validation. **Xiaojun Bian:** Supervision, Methodology, Writing – review & editing. **Qing Tao:** Software, Data curation, Validation. **Gang Liu:** Resources, Supervision. **Juan Yan:** Conceptualization, Project administration, Resources, Supervision, Funding acquisition, Writing – review & editing.

Table 1
Detection of KAN in real food samples using TdT-based colorimetric aptasensor.

Sample	Added (nM)	Found (nM)	Recovery (%)	RSD (%)
Milk	0	ND		
Milk	0.5	0.538	107.6	3.67
Milk	1	0.974	97.4	4.39
Milk	5	4.691	93.8	1.22
Honey	0	ND		
Honey	0.5	0.487	97.4	3.68
Honey	1	0.964	96.4	2.16
Honey	5	5.389	107.8	2.52

ND: Not determined.

Declaration of Competing Interest

The authors declare that they have no known competing financial interests or personal relationships that could have appeared to influence the work reported in this paper.

Acknowledgements

This work was supported by the National Natural Science Foundation of Chin (Nos. 21775102, 21775104, 22074093), Natural Science Foundation of Shanghai (No. 20ZR1424100).

Appendix A. Supplementary data

Supplementary data to this article can be found online at https://doi.org/10.1016/j.foodchem.2022.132072.

References

Bai, Z. H., Chen, Y., Li, F., Zhou, Y. L., Yin, H. S., & Ai, S. Y. (2019). Electrochemical aptasensor for sulfadimethoxine detection based on the triggered cleavage activity of nuclease P1 by aptamer-target complex. *Talanta, 204*, 409–414. https://doi.org/10.1016/j.talanta.2019.06.035

Birader, K., Kumar, P., Tammineni, Y., Barla, J. A., Reddy, S., & Suman, P. (2021). Colorimetric aptasensor for on-site detection of oxytetracycline antibiotic in milk. *Food Chemistry, 356*, Article 129659. https://doi.org/10.1016/j.foodchem.2021.129659

Cheng, R. J., Liu, S. Y., Shi, H. J., & Zhao, G. H. (2018). A highly sensitive and selective aptamer-based colorimetric sensor for the rapid detection of PCB 77. *Journal of Hazardous Materials, 341*, 373–380. https://doi.org/10.1016/j.jhazmat.2017.07.057

Cheng, S. T., Liu, H. M., Zhang, H., Chu, G. L., Guo, Y. M., & Sun, X. (2020). Ultrasensitive electrochemiluminescence aptasensor for kanamycin detection based on silver nanoparticle-catalyzed chemiluminescent reaction between luminol and hydrogen peroxide. *Sensors and Actuators B: Chemical, 304*, 127367–127373. https://doi.org/10.1016/j.snb.2019.127367

Cheng, S. T., Zhang, H., Huang, J. C., Xu, R., Sun, X., & Guo, Y. M. (2020). Highly sensitive electrochemiluminescence aptasensor based on dual-signal amplification strategy for kanamycin detection. *Science of the Total Environment, 737*, 139785–139792. https://doi.org/10.1016/j.scitotenv.2020.139785

Commission, E. (2010). Commission Regulation (EU) No. 37/2010 of 22 December 2009: on Pharmacologically Active Substances and Their Classification Regarding Maximum Residue Limits in Foodstuffs of Animal Origin. *Official Journal of the European Union*, 1-72.

Du, Y. M., Zhou, Y. Y., Wen, Y. L., Bian, X. J., Xie, Y. Y., Zhang, W. J., … Yan, J. (2019). Multiplexed aptasensing of food contaminants by using terminal deoxynucleotidyl transferase-produced primer-triggered rolling circle amplification: Application to the colorimetric determination of enrofloxacin, lead (II), Escherichia coli O157:H7 and tropomyosin. *Microchimica Acta, 186*(12), 840–849. https://doi.org/10.1007/s00604-019-3935-2

Feng, D. F., Tan, X. C., Wu, Y. Y., Ai, C. H., Luo, Y. N., Chen, Q. Y., & Han, H. Y. (2019). Electrochemiluminecence nanogears aptasensor based on MIL-53(Fe)@CdS for multiplexed detection of kanamycin and neomycin. *Biosensors and Bioelectronics, 129*, 100–106. https://doi.org/10.1016/j.bios.2018.12.050

Guo, J., Yuan, C. J., Yan, Q., Duan, Q. Y., Li, X. L., & Yi, G. (2018). An electrochemical biosensor for microRNA-196a detection based on cyclic enzymatic signal amplification and template-free DNA extension reaction with the adsorption of methylene blue. *Biosensors and Bioelectronics, 105*, 103–108. https://doi.org/10.1016/j.bios.2018.01.036

Ha, N. R., Jung, I. P., Kim, S. H., Kim, A. R., & Yoon, M. Y. (2017). Paper chip-based colorimetric sensing assay for ultra-sensitive detection of residual kanamycin. *Process Biochemistry (Barking, London, England), 62*, 161–168.

He, L., Shen, Z., Cao, Y., Li, T., Wu, D., Dong, Y., & Gan, N. (2019). A microfluidic chip based ratiometric aptasensor for antibiotic detection in foods using stir bar assisted

sorptive extraction and rolling circle amplification. *Analyst, 144*(8), 2755–2764. https://doi.org/10.1039/C9AN00106A

Li, C., Zhang, Y. Y., Eremin, S. A., Yakup, O., Yao, G., & Zhang, X. Y. (2017). Detection of kanamycin and gentamicin residues in animal-derived food using IgY antibody based ic-ELISA and FPIA. *Food Chemistry, 227*, 48–54. https://doi.org/10.1016/j.foodchem.2017.01.058

Li, J., Liu, Y., Lin, H., Chen, Y., Liu, Z., Zhuang, X., Tian, C., Fu, X., & Chen, L. (2021). Label-free exonuclease I-assisted signal amplification colorimetric sensor for highly sensitive detection of kanamycin. *Food Chemistry, 347*, Article 128988. https://doi.org/10.1016/j.foodchem.2020.128988

Li, S. T., Li, G. S., Du, Z. H., Zhu, L. J., Tian, J. J., Luo, Y. B., & Xu, W. T. (2019). The ultra-sensitive visual biosensor based on thermostatic triple step functional nucleic acid cascade amplification for detecting Zn^{2+}. *Food Chemistry, 290*, 95–100. https://doi.org/10.1016/j.foodchem.2019.03.134

Lin, X. X., Su, J. L., Lin, H. G., Sun, X. Y., Liu, B., Kankala, R. K., & Zhou, S. F. (2019). Luminescent carbon nanodots based aptasensors for rapid detection of kanamycin residue. *Talanta, 202*, 452–459. https://doi.org/10.1016/j.talanta.2019.04.075

Liu, M., Yang, Z. Q., Li, B. X., & Du, J. X. (2021). Aptamer biorecognition-triggered hairpin switch and nicking enzyme assisted signal amplification for ultrasensitive colorimetric bioassay of kanamycin in milk. *Food Chemistry, 339*, 128059–128064. https://doi.org/10.1016/j.foodchem.2020.128059

Park, C. H., Vo, C. L. N., Kang, T. H., Oh, E. C., & Lee, B. J. (2015). New method and characterization of self-assembled gelatin-oleic nanoparticles using a desolvation method via carbodiimide/N-hydroxysuccinimide (EDC/NHS) reaction. *European Journal of Pharmaceutics and Biopharmaceutics, 89*, 365–373. https://doi.org/10.1016/j.ejpb.2014.12.002

Perez, J. J., & Chen, C. Y. (2018). Rapid detection and quantification of aminoglycoside phosphorylation products using direct-infusion high-resolution and ultra-high-performance liquid chromatography/mass spectrometry. *Rapid Communications in Mass Spectrometry: Rcm., 32*(20), 1822–1828. https://doi.org/10.1002/rcm.8241

Qiu, X., Wang, S. S., Miao, S. S., Suo, H. B., Xu, H. J., & Hu, Y. (2020). Co-immobilization of laccase and ABTS onto amino-functionalized ionic liquid-modified magnetic chitosan nanoparticles for pollutants removal. *Journal of Hazardous Materials, 401*, 123353–123363. https://doi.org/10.1016/j.jhazmat.2020.123353

Ramezani, M., Danesh, N. M., Lavaee, P., Abnous, K., & Taghdisi, S. M. (2016). A selective and sensitive fluorescent aptasensor for detection of kanamycin based on catalytic recycling activity of exonuclease III and gold nanoparticles. *Sensors and Actuators B: Chemical, 222*, 1–7. https://doi.org/10.1016/j.snb.2015.08.024

Robati, R. Y., Arab, A., Ramezani, M., Langroodi, F. A., Abnous, K., & Taghdisi, S. M. (2016). Aptasensors for quantitative detection of kanamycin. *Biosensors and Bioelectronics, 82*, 162–172. https://doi.org/10.1016/j.bios.2016.04.011

Sadasivam, M., Sakthivel, A., Nagesh, N., Hansda, S., Veerapandian, M., Alwarappan, S., & Manickam, P. (2020). Magnetic bead-amplified voltammetric detection for carbohydrate antigen 125 with enzyme labels using aptamer-antigen-antibody sandwiched assay. *Sensors and Actuators B: Chemical, 312*, 127985–127993. https://doi.org/10.1016/j.snb.2020.127985

Shen, R. D., Zhang, J., Huang, W. X., Wu, S. Y., Li, G. K., Zou, S. Y., & Ling, L. S. (2021). Dynamic light scattering and fluorescence dual-signal sensing of cancer antigen-125 via recognition of the polymerase chain reaction product with gold nanoparticle probe. *Analytica Chimica Acta, 1145*, 87–94. https://doi.org/10.1016/j.aca.2020.11.005

Song, S. P., Wang, L. H., Li, J., Fan, C. H., & Zhao, J. L. (2008). Aptamer-based biosensors. *Trends in Analytical Chemistry, 27*(2), 108–117. https://doi.org/10.1016/j.trac.2007.12.004

Tian, F. Y., Zhou, J., Jiao, B. N., & He, Y. (2019). A nanozyme-based cascade colorimetric aptasensor for amplified detection of ochratoxin A. *Nanoscale, 11*(19), 9547–9555. https://doi.org/10.1039/c9nr02872b

Tian, R., Ji, J. Y., Zhou, Y. Y., Du, Y. M., Bian, X. J., Zhu, F. L., … Yan, J. (2020). Terminal-conjugated non-aggregated constraints of gold nanoparticles on lateral flow strips for mobile phone readouts of enrofloxacin. *Biosensors and Bioelectronics, 160*, 112218–112226. https://doi.org/10.1016/j.bios.2020.112218

Tuerk, C., & Gold, L. (1990). Systematic evolution of ligands by exponential enrichment: RNA ligands to bacteriophage T4 DNA polymerase. *Science, 249*(4968), 505–510. https://doi.org/10.1126/science.2200121

Wang, Y., Gan, N., Zhou, Y., Li, T. H., Hu, F. T., Cao, Y. T., & Chen, Y. J. (2017). Novel label-free and high-throughput microchip electrophoresis platform for multiplex antibiotic residues detection based on aptamer probes and target catalyzed hairpin assembly for signal amplification. *Biosensors and Bioelectronics, 97*, 100–106. https://doi.org/10.1016/j.bios.2017.05.017

Wu, Y. Y., Huang, P., & Wu, F. Y. (2020). A label-free colorimetric aptasensor based on controllable aggregation of AuNPs for the detection of multiplex antibiotics. *Food Chemistry, 304*, Article 125377. https://doi.org/10.1016/j.foodchem.2019.125377

Xu, Y. Y., Han, T., Li, X. Q., Sun, L. H., Zhang, Y. J., & Zhang, Y. S. (2015). Colorimetric detection of kanamycin based on analyte-protected silver nanoparticles and aptamer-selective sensing mechanism. *Analytica Chimica Acta, 891*, 298–303. https://doi.org/10.1016/j.aca.2015.08.013

Yan, C., Zhang, J., Yao, L., Xue, F., Lu, J. F., Li, B. G., & Chen, W. (2018). Aptamer-mediated colorimetric method for rapid and sensitive detection of chloramphenicol in food. *Food Chemistry, 260*, 208–212. https://doi.org/10.1016/j.foodchem.2018.04.014

Yan, J., Hu, C., Wang, P., Zhao, B., Ouyang, X., Zhou, J., Liu, R., He, D., Fan, C., & Song, S. (2015). Growth and Origami Folding of DNA on Nanoparticles for High-Efficiency Molecular Transport in Cellular Imaging and Drug Delivery. *Angewandte Chemie International Edition, 54*(8), 2431–2435. https://doi.org/10.1002/anie.201408247

Yan, J., Song, S. P., Li, B., Zhang, Q. Z., Huang, Q., Zhang, H., & Fan, C. H. (2010). An on-nanoparticle rolling-circle amplification platform for ultrasensitive protein detection in biological fluids. *Small, 6*(22), 2520–2525. https://doi.org/10.1002/smll.201001220

Zhang, L. L., Zhu, C. C., Chen, C. B., Zhu, S. H., Zhou, J., Wang, M. L., & Shang, P. P. (2018). Determination of kanamycin using a molecularly imprinted SPR sensor. *Food Chemistry, 266*, 170–174. https://doi.org/10.1016/j.foodchem.2018.05.128

Zhang, X. P., Wang, J. J., Wu, Q. H., Li, L., Wang, Y., & Yang, H. L. (2019). Determination of Kanamycin by High Performance Liquid Chromatography. *Molecules, 24*(10), 1902–1925. https://doi.org/10.3390/molecules24101902

Zhang, Z. X., Wang, Z. J., Wang, X. L., & Yang, X. R. (2010). Magnetic nanoparticle-linked colorimetric aptasensor for the detection of thrombin. *Sensors and Actuators B: Chemical, 147*(2), 428–433. https://doi.org/10.1016/j.snb.2010.02.013

Zhou, C., Zou, H., Sun, C., & Li, Y. (2021). Recent advances in biosensors for antibiotic detection: Selectivity and signal amplification with nanomaterials. *Food Chemistry, 361*, Article 130109. https://doi.org/10.1016/j.foodchem.2021.130109

Zhou, Y. L., Li, F., Wu, H. W., Chen, Y., Yin, H. S., Ai, S. Y., & Wang, J. (2019). Electrochemical aptasensing strategy for kanamycin detection based on target-triggered single-strand DNA adsorption on MoS_2 nanosheets and enzymatic signal amplification. *Sensors and Actuators B: Chemical, 296*, 126664–126670. https://doi.org/10.1016/j.snb.2019.126664

Zhu, X., Tang, L., Wang, J. J., Peng, B., Ouyang, X. L., Tan, J. S., … Tang, J. L. (2021). Enhanced peroxidase-like activity of boron nitride quantum dots anchored porous CeO_2 nanorods by aptamer for highly sensitive colorimetric detection of kanamycin. *Sensors and Actuators B: Chemical, 330*, 129318–129326. https://doi.org/10.1016/j.snb.2020.129318

Zhu, Y., Chandra, P., Song, K. M., Ban, C., & Shim, Y. B. (2012). Label-free detection of kanamycin based on the aptamer-functionalized conducting polymer/gold nanocomposite. *Biosensors and Bioelectronics, 36*(1), 29–34. https://doi.org/10.1016/j.bios.2012.03.034